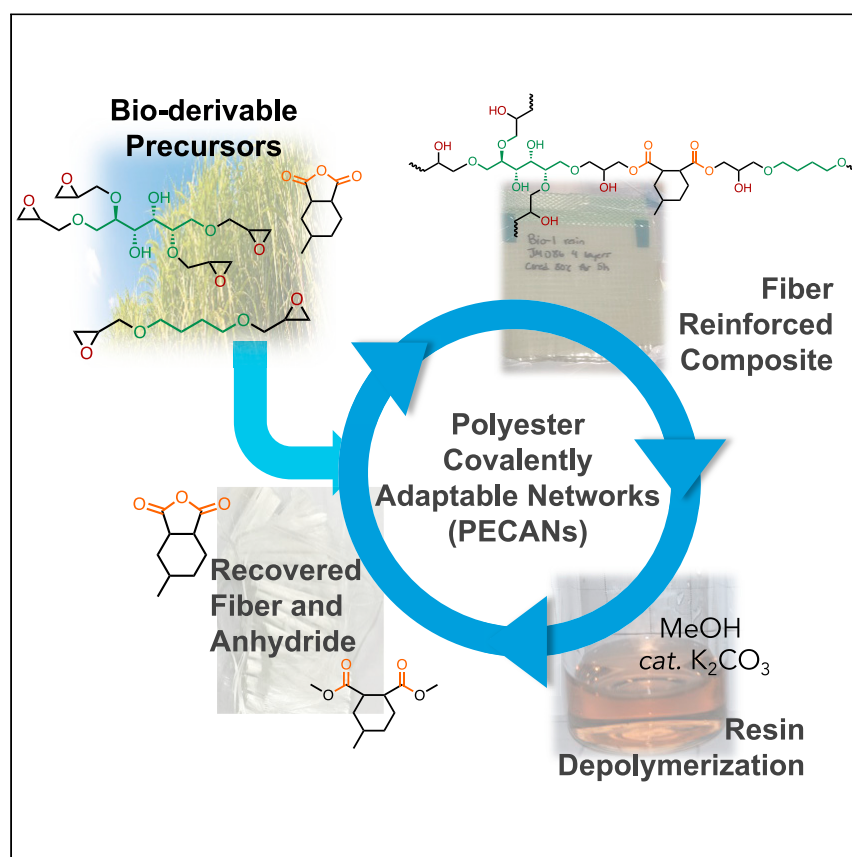


Article

Synthesis, characterization, and recycling of bio-derivable polyester covalently adaptable networks for industrial composite applications



Wind turbines are crucial materials for today's energy economy; however, their blades are non-recyclable due to the epoxy-amine thermosetting resins employed. To enable recyclability, circularity, and ideally decarbonization in the manufacture of wind turbine blades, we designed a bio-derivable epoxy anhydride resin, named a polyester covalently adaptable network (PECAN), in analogy to today's epoxy-amine resins. When used in a 1-kg fiber-reinforced plastic, the PECAN resins possess comparable manufacturing and thermomechanical performance to the epoxy-amine resins while being recyclable.

Chen Wang, Avantika Singh, Erik G. Rognerud, ..., Robert D. Allen, Gregg T. Beckham, Nicholas A. Rorrer

gregg.beckham@nrel.gov (G.T.B.)
nicholas.rorrer@nrel.gov (N.A.R.)

Highlights

Recyclable epoxy-anhydride resins are designed in analogy to epoxy amine resins

Recyclable resins can be manufactured in the same way as non-recyclable resins

The recyclable resins exhibit comparable performance in fiber-reinforced plastics

Analysis reveals up to a 40% reduction in GHG emissions and a comparable cost

Wang et al., Matter 7, 550–568

February 7, 2024 © 2023 National Renewable Energy Laboratory (NREL) and The Author(s).
Published by Elsevier Ltd.

<https://doi.org/10.1016/j.matt.2023.10.033>

**Demonstrate**

Proof-of-concept of performance with intended application/response



Article

Synthesis, characterization, and recycling of bio-derivable polyester covalently adaptable networks for industrial composite applications

Chen Wang,^{1,2,7,8} Avantika Singh,^{2,3,8} Erik G. Rognerud,^{1,2,8} Robynne Murray,^{4,8} Grant M. Musgrave,^{4,7} Morgan Skala,^{1,2} Paul Murdy,⁴ Jason S. DesVeaux,^{2,3} Scott R. Nicholson,^{2,5} Kylee Harris,^{2,3} Richard Canty,⁶ Fabian Mohr,⁶ Alison J. Shapiro,^{1,2} David Barnes,⁴ Ryan Beach,⁴ Robert D. Allen,^{1,2} Gregg T. Beckham,^{1,2,*} and Nicholas A. Rorrer^{1,2,9,*}

SUMMARY

Fiber-reinforced polymers (FRPs) are critical for energy-relevant applications such as wind turbine blades. Despite this, the end-of-life options for FRPs are limited as they are permanently cross-linked thermosets. To enable the circularity of FRPs, we formulated a bio-derivable polyester covalently adaptable network (PECAN), sometimes referred to as a polyester vitrimer, to manufacture FRPs at >1 kg scale, which is accomplished as the resin is infusible (175–425 cP at 25°C viscosity), can be cured at 80°C within 5 h and is depolymerizable via methanolysis yielding high-quality fibers and recoverable hardener. The FRPs exhibit a transverse tensile modulus comparable with today's wind relevant FRPs (10.4–11.9 GPa). Modeling estimates a resin minimum selling price of \$2.28/kg and, relative to an epoxy-amine resin, PECAN manufacture requires 19%–21% less supply chain energy and emits 33%–35% less greenhouse gas emissions. Overall, this study suggests that re-designed thermosets can yield beneficial circularity.

INTRODUCTION

Fiber-reinforced polymers (FRPs) are widely employed as structural components in automobiles, aerospace, wind turbine blades, and other applications that require robust performance across long material lives.^{1–4} Typically, FRPs are formulated from a fiber (e.g., glass or carbon), which endows high strength-to-weight ratios,⁴ and a thermosetting polymer, which provides stiffness. Together, these combined properties endow the overall structural integrity of the composite. While these thermosets can be formulated using multiple chemistries, epoxy resins synthesized from epoxy monomers (e.g., bisphenol A diglycidal ether [BADGE], hexanediol diglycidal ether [HDGE], etc.) and amine “hardeners” are the most widely used.^{1,5} Epoxy-amine resins exhibit robust mechanical integrity due to their cross-linked structure, recalcitrance to chemical corrosion due to the stable C–N bonds, and facile reaction during manufacturing due to the favorable kinetics of the epoxy ring opening. However, the recalcitrance of the thermoset network and inter-unit linkages together lead to minimal end-of-life options for FRPs. Indeed, it is estimated that the cumulative wind turbine blade waste alone will reach 43 million tons globally by 2050⁶ if no viable end-of-life solutions are developed.

This linear flow of materials presents both an environmental problem and lost economic potential. To enable cost-effective circularity of FRPs, it is necessary to remove

PROGRESS AND POTENTIAL

Fiber-reinforced polymers (FRPs) can contribute to a decarbonized society by light-weighting transportation applications and enabling robust wind turbines. Despite this, the manufacture and inability of FRP component parts to be reused contributes to growing material waste and continued greenhouse gas emissions. To decarbonize composite manufacturing, it is possible to redesign the thermosetting polymer used in these composites to be sourced from bio-derivable feedstocks and to be inherently recyclable while exhibiting the same performance and manufacturing characteristics. Within the present work, we accomplish this goal by leveraging bio-based epoxies and anhydrides to make PECANs that maintain the requisite performance while being depolymerizable using inexpensive reagents, resulting in completely recyclable resins.



the thermosetting polymer from the fiber reinforcement. For epoxy-amine chemistries, pyrolysis or chemo-catalytic approaches can be applied. Pyrolysis does not recover the original monomers and results in char formation, which complicates fiber re-use due to changes at the fiber interface.⁷ Recently, selective depolymerization has been shown to successfully recover the fibers post-depolymerization and select monomers.^{8–10} While methods to depolymerize today's resins are needed, there is a complementary long-term opportunity to redesign the thermosetting network itself with dynamic covalent chemistries to aid in the recycling of future FRPs. Dynamic covalent chemistries used in thermosetting materials are known as covalent adaptable networks (CANs)¹¹ or vitrimers.^{12,13} Cross-links between polymer chains in these materials can be cleaved through known reactions typically using an excess of a reactive species and has been demonstrated in polyesters,¹⁴ polydiketoimines,^{15–17} polyimines,¹⁸ polyureas,¹⁹ polythioesters,²⁰ and polythiourethanes.²¹

While CAN-based thermosets can be recycled, there are multiple performance considerations to make an FRP material viable industrially for high-performance applications, such as those required for the manufacture of a wind turbine blade. Importantly, the resins would ideally be compatible with existing manufacturing infrastructure. For the wind industry, the resins would be amenable to vacuum-assisted resin transfer molding (VARTM) to infuse large stacks of fibers of varying geometries prior to cure.²² For this manufacturing method, the resins must be a liquid at room temperature, exhibit low viscosity, and have a pot-life that is sufficiently long so as to not cure within the infusion lines or before the fibers are fully saturated with resin. Additional considerations include a cure temperature of less than 100°C, controllable cure exotherms, and moderate cure times, among others. These considerations are mainly driven by the need to limit the temperature that the composite tools are exposed to and to minimize the manufacturing time for large composite structures, as this largely drives the manufacturing costs.²³

In this work, we developed FRPs with a recyclable thermoset resin that implements dynamic covalent chemistries, namely, polyester CAN (PECAN) formed from the reaction of epoxies and anhydrides. Here, we refer to the materials as covalently adaptable networks as they have been previously demonstrated to be so with and without catalyst; however, they can also be referred to as vitrimers.^{24–26} Epoxy-anhydride resins can be bio-derivable,^{27,28} which potentially can reduce the associated greenhouse gas (GHG) emissions from their manufacture,²⁹ while providing ester bonds that can be cleaved with multiple catalytic methods.^{30–33} The epoxy-anhydride chemistry was designed in analogy to an industry-preferred epoxy-amine resin with a rigid epoxy component, a reactive diluent compound, and a cycloaliphatic hardener, all of which can be derived from carbohydrates. The performance of the epoxy-anhydride resin was compared with a wind industry-relevant epoxy-amine resin in terms of cure conditions, neat resin performance, FRP performance, recyclability, economics, and environmental impacts. The performance of the epoxy-anhydride resin was comparable with the epoxy-amine resins, while being recyclable in a low-temperature catalytic process at all scales studies up to one kg. Finally, economic and cradle-to-gate supply chain analysis were performed, which estimated a comparable price between the epoxy-amine and epoxy-anhydride resin with a 21%–23% decrease in GHG emissions.

RESULTS

Baseline epoxy-amine resin and PECAN resin formulations

For this work, we first developed a baseline epoxy-amine (BEA) resin with a known composition representative of resins and cure chemistries currently used in wind

¹Renewable Resources and Enabling Sciences Center, National Renewable Energy Laboratory, Golden, CO 80401, USA

²BOTTLE Consortium, Golden, CO 80401, USA

³Catalytic Carbon Transformation and Scale-up Center, National Renewable Energy Laboratory, Golden, CO 80401, USA

⁴National Wind Technology Center, National Renewable Energy Laboratory, Boulder, CO 80401, USA

⁵Strategic Energy Analysis Center, National Renewable Energy Laboratory, Golden, CO 80401, USA

⁶David H. Koch School of Chemical Engineering Practice, Massachusetts Institute of Technology, Cambridge, MA 02139, USA

⁷Present address: Department of Materials Science and Engineering, University of Utah, Salt Lake City, UT 84112, USA

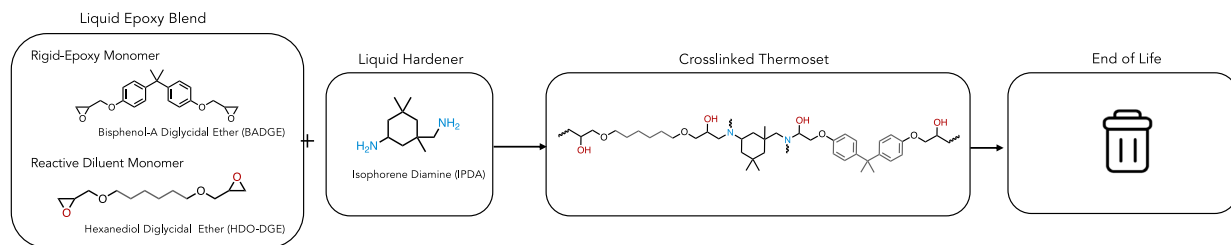
⁸These authors contributed equally

⁹Lead contact

*Correspondence: gregg.beckham@nrel.gov (G.T.B.), nicholas.rorrer@nrel.gov (N.A.R.)

<https://doi.org/10.1016/j.matt.2023.10.033>

A Baseline epoxy-amine resin



B Polyester covalently adaptable networks (PECANs)

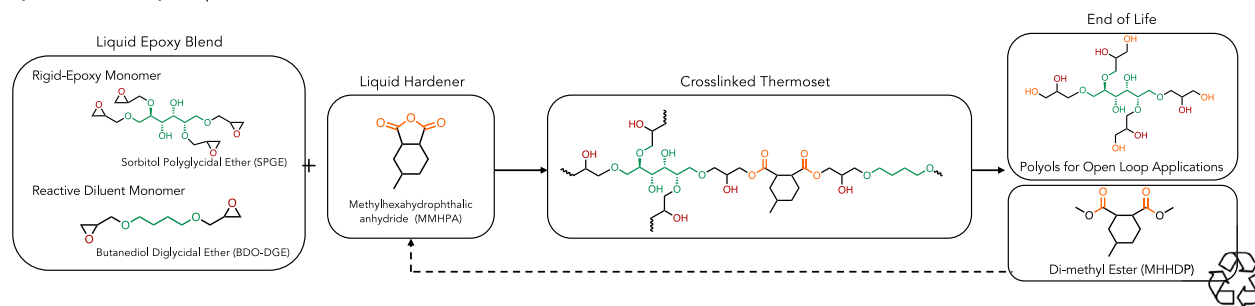


Figure 1. BEA and PECAN resin formulations

(A) Typical epoxy-amine formulation, synthesis, and end of life, including the monomers used in our BEA resin to resemble an industrial resin (Hexion). (B) The monomers of our PECAN resin used in this work and their respective role relative to the epoxy amine resin.

turbine blades. A typical resin used in the wind industry today consists of an epoxy component, such as Hexion RIMR-135, and an amine hardener, such as RIMH-1366, which taken together comprise the infusible resin for wind turbines.³⁴ After chemical curing, the resultant thermoset network exhibits both C–N bonds and β -hydroxyl groups, which overall yield materials with a high degree of chemical resistance, thermomechanical properties for high-performance applications, and strong adhesion to reinforcements. According to the industry specification sheets, resin components contain BADGE, HDGE, isophorone diamine (IPDA), aminoethylpiperazine, and poly(oxypropylene) diamine, along with other proprietary components. For the BEA resin, we simplified our formulation to BADGE (a rigid epoxy), HDGE (a reactive diluent epoxy), and IPDA (a multifunctional hardener) (Figure 1A).

To design a recyclable thermoset resin, we aimed to replace the amine hardener with an anhydride hardener to produce a resin we dubbed a PECAN. By replacing the amine with an anhydride, the resulting materials are polyesters, which can be more readily depolymerized. For the epoxy-anhydride resin, we used building blocks that could be sourced from bio-based feedstocks. For the epoxy components, we used sorbitol poly-glycidyl ether (SPGE) and butanediol diglycidyl ether (BDGE), which mimic the rigid monomer and reactive diluent monomer of the BEA formula, respectively. Sorbitol can be obtained from glucose^{35,36} and 1,4-butanediol (1,4-BDO) can be obtained through an engineered microbe from direct fermentation of sugars^{37,38} or from reduction of bio-based succinic acid.^{39–41} The epoxies can thus be formed by reacting the alcohols with bio-based epichlorohydrin obtained from waste glycerol. We selected methylhexahydrophthalic anhydride (MHHPA) as our hardener (Figure 1B), which can be obtained from the Diels-Alder condensation of isoprene and maleic anhydride, both of which are obtainable from bio-based feedstocks.^{42,43} Throughout this study, we use commercially available monomers; however, there are companies actively

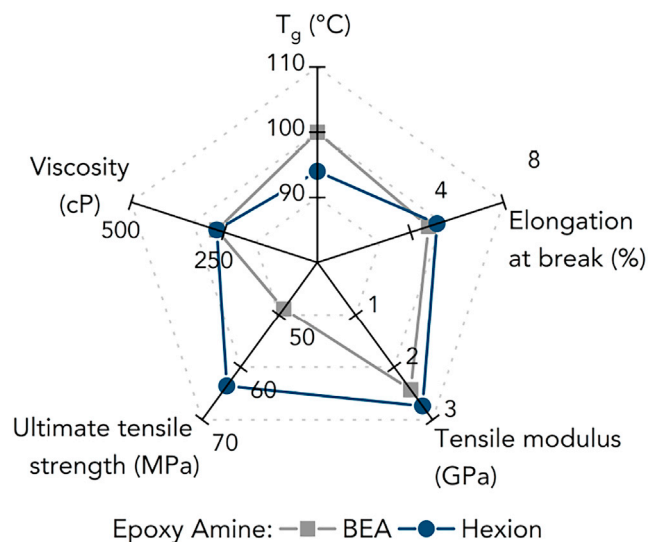


Figure 2. Hexion and BEA resin formulations

The properties of the neat BEA resin relative to an industry standard neat Hexion resin demonstrating comparable or enhanced performance. Numerical data are provided in [Table S2](#).

working on the scale-up of all the component parts of the resin, as noted in [Table S1](#).

After the selection of components, we tested the BEA resin relative to the Hexion resin. We found that a mixture with an equal mass of BADGE and HDGE reacted with a stoichiometric ratio of IPDA (where equal stoichiometry is defined as one reactive amine proton to one epoxy moiety) was a suitable benchmark for the commercial Hexion resin, as shown in [Figure 2](#), with numerical data presented in [Table S2](#). Akin to other epoxy-amine resins, the BEA resin can be manufactured using VARTM because of its low viscosity (<400 cP at 25°C) that enables infusion, an adequate operation window between resin mixing and the polymerization reactions (>2 h at 25°C) to allow for infusion, and a cure at accessible temperature for moderate times (<100°C for <8 h).

Both the BEA resin and the commercial Hexion (RIMR-135/RIMH-1366) resins exhibit similar thermomechanical properties, with a glass transition temperature (T_g) between 94°C and 100°C as measured by differential scanning calorimetry (DSC). The viscosity is comparable between the two uncured epoxy amine resins at 500 cP. The only difference in the material properties manifests in the tensile testing (ASTM D638) in which the tensile modulus and elongation at break are comparable, but the ultimate tensile strength (UTS) is lower for the BEA resin. The lower UTS is attributed to the Hexion resin containing unknown additives that strengthen the resin.

After the formation of the BEA resin for comparison, we developed three PECAN compositions for this work. The PECAN formulations were dubbed SPGE-39, SPGE-33, and SPGE-28. Each formulation was made by assuming ideal epoxy stoichiometry for the BDGE and SPGE, two and four, respectively, and formulating a stoichiometric ratio between the epoxy components and the anhydride hardener (one epoxide to one anhydride group). In the naming convention, the number refers to the weight percentage of SPGE, which are given in [Table S3](#). This was done as properties, such as stiffness and glass transition, are expected to scale with SPGE

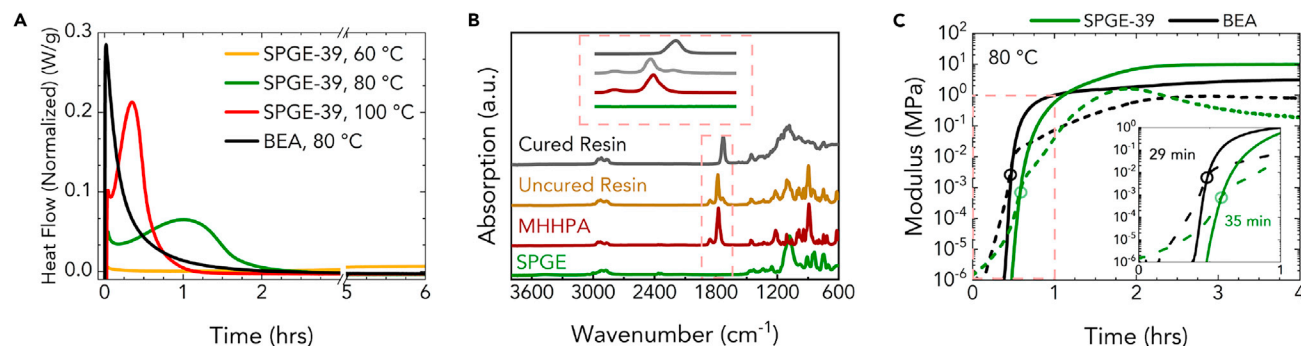


Figure 3. Cure kinetics comparison of the BEA and PECAN SPGE-39 resins

(A) DSC results for the BEA and PECAN SPGE-39 resin curing reactions with 2-ethyl-4-methylimidazole (2,4-EMI) as the catalyst. The samples (~10 mg) were loaded in the DSC at room temperature and rapidly heated (20°C/min) to various the target isothermal dwell temperature for 6 h. (B) FTIR spectra of the PECAN monomers, uncured resin, and cured resin. After the 5-h cure at 80°C, the disappearance of the anhydride peak and the formation of ester peaks for the PECAN resin demonstrate complete conversion. (C) *In situ* rheology measurements of the polymerization of the BEA and PECAN SPGE-39 at 80°C with 2,4-EMI. The storage and loss moduli for the BEA (black) and PECAN SPGE-39 (green) are shown in solid lines and dotted lines, respectively. The gel points are indicated with a circle.

content. It is important to note that this method for calculating stoichiometry may over-estimate the epoxy content, and therefore the extent of cross-linking, as commercial epoxies report a range of epoxy content known as the epoxy equivalent weight.^{1,5,44,45} Of equal importance is that every formulated resin exhibits a viscosity of less than 500 cP, making them amenable to the VARTM process. These PECAN resins, designed in analogy to a representative epoxy amine resin, were used throughout the remainder of the study.

Resin cure kinetics

After formulation, we investigated the cure properties of the PECAN SPGE-39 resin relative to the BEA resin with DSC and rheology measurements. For studying resin cure kinetics, SPGE-39 was selected as it possesses the highest amount of cross-linking and thus should be the slowest polymer to cross-link relative to SPGE-33 and SPGE-28. Initially, the polymerization with 2-ethyl-4-methylimidazole as a catalyst at a loading of 1 wt % as a catalyst was conducted in a DSC to monitor the exothermic reaction as a function of temperature and time (Figure 3A). Polymerization progress can be monitored by observing the heat flow as a function of time and when there is no more residual exotherm (i.e., the heat flow returns to zero), the reaction was considered complete.⁴⁶ At 80°C, the PECAN and BEA resins take 3 h and 1 h to complete, respectively.

Further investigation into the PECAN resin demonstrates that the reaction time varies with temperature: namely, at 100°C, the reaction is completed within 1 h, while at 60°C, the reaction exhibited minimal exothermic behavior and did not complete within 6 h. After DSC, the completion of the polymerization reaction was confirmed by Fourier transform infrared (FTIR) spectroscopy (Figure 3B). The cure completion is evident by the disappearance of the anhydride carbonyl stretch at 1,780 cm⁻¹, originally seen in both MHHPA and the uncured PECAN resin, and the appearance of an ester carbonyl stretch at 1,730 cm⁻¹ in the cured resin.

Additionally, rheology was used to measure the pot life of the SPGE-39 PECAN resin and the BEA resin. To do this, we conducted standard isothermal oscillatory rheology with 0.1% strain at 1 Hz frequency and 80°C. The gel point, or the point where the storage and loss moduli cross one another, was determined using this

technique. The time it takes to reach the gel point reflects how long the resin is considered a liquid at a given temperature. Figure 3C provides the storage (solid lines) and loss modulus (dashed lines) of both the PECAN STGE-39 (green) and the BEA (black) resins. The gel time is 35 and 29 min for the PECAN and BEA resins, respectively. The storage modulus for the BEA resin plateaus in less than 1 h, while the PECAN resin plateaus in less than 3 h, indicating that the cure is complete and corroborating the DSC results. As the PECAN resin exhibited a higher storage modulus and lower loss modulus than the BEA resin via shear rheology, this result is an indicator that the PECAN resin may result in strong composites with robust fiber adhesion.^{47,48} With these results, we determined that, for both the epoxy-anhydride and epoxy-amine resins, a cure temperature of 80°C for 5 h would be sufficient to ensure complete conversion for subsequent tests.

Cured resin thermomechanical performance

After the determination of the cure kinetics, cured neat resin samples (i.e., samples of the polymer itself with no reinforcement or additives) were prepared to assess their thermomechanical performance relative to the BEA resin using dynamic mechanical analysis (DMA) and tensile testing. DMA was used to assess both the thermal properties of the cured resins and ensure they are cross-linked. Meanwhile, tensile testing was used to determine the tensile behavior of the materials. Additionally, DSC and thermogravimetric analysis (TGA) were used as supplemental thermal characterizations.

DMA bars of dimensions 12.8 mm × 17.5 mm × 2 mm (width × length × depth) were prepared and then subjected to single cantilever oscillatory experiment (1 Hz). Experiments were conducted from room temperature to 180°C at a ramp rate of 3°C/min. Resin bars were first annealed in the DMA with a preliminary temperature ramp to relieve stresses imparted during cure and sample loading. Successive temperature ramps were run until the peak $\tan \delta$ stabilized (<1°C on successive runs). This process effectively post-cured the DMA samples as well. Figure S1 shows the storage modulus of the neat PECAN resins before and after post cure, demonstrating a consistent storage and plateau modulus. The thermoset behavior of the resins was also confirmed, as there are no signs of flow (i.e., no decrease in storage modulus at elevated temperatures) and consistent plateau moduli over multiple heating cycles.

Thermal analysis of the $\tan \delta$ thermograms (Figure S1) was used to determine the T_g of the PECAN resins by analyzing the temperature at which the $\tan \delta$ is at a maximum. Analysis of the fully cured resin relative to the first temperature ramp shows that the final T_g is limited by the cure temperature such that SPGE-39 has a final T_g of 120°C, while the first scan yields a T_g of 100°C. Therefore, the final scan was used for analysis. For the PECAN resins, the T_g increases with increasing SPGE content and thus increasing cross-link density accompanied by decreasing reactive diluent. Specifically, the SPGE-39, SPGE-33, and SPGE-28 possess T_g values of 120°C ± 3°C, 103°C ± 3°C, and 93°C ± 3°C, respectively (Figures 4A–4C, with numerical data provided in Table S4), comparable with the BEA resin with a T_g of 100°C ± 3°C. In addition to T_g , the degradation temperature of the resins was measured by TGA at a heating ramp of 20°C/min under flowing nitrogen. The cured PECAN resins exhibit similar thermal stability, akin to the BEA resins with 5% degradation temperature (T_d 5%) of 315°C ± 10°C for the PECAN resin and 336°C ± 10°C for the BEA resin (Figure S2). Taken together, these results indicate that the PECAN resin can operate under similar thermal and mechanical stress as the epoxy-amine resins.

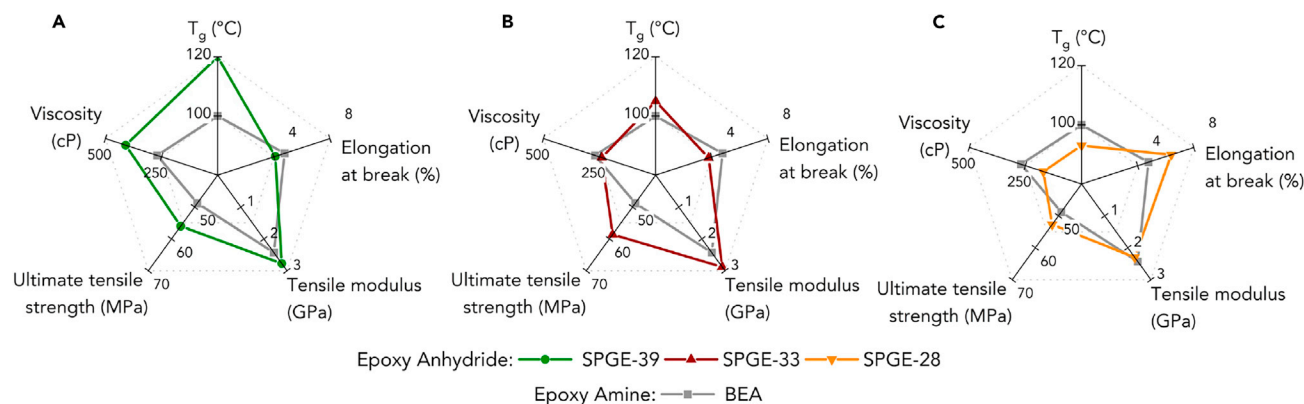


Figure 4. Cured neat resin thermomechanical performance

(A–C) Spider charts show the T_g , viscosity, UTS, tensile modulus, and percent elongation at break for neat resin samples of (A) SPGE-39, (B) SPGE-33, and (C) SPGE-28. All spider charts also show comparisons to cured BEA resin. The T_g was analyzed via DMA, viscosity was analyzed via a rheometer, and tensile data were collected on a universal testing machine. Figure S1 provides representative thermograms and stress-strain plots, while numerical data for the figures are provided in Table S4.

After thermal and DMA characterization, ASTM D638 Type IV dog bones were made for tensile testing, which was conducted in triplicate for each resin formulation. Figure S1 also provides representative stress-strain curves of the PECAN resins relative to BEA and Table S4 provides the numerical values. In general, the tensile performance of the three PECAN formulations and the BEA resin are similar. The tensile performance of the three PECAN formulations and the BEA resin are similar. The tensile modulus and UTS were found to vary insignificantly for the SPGE-39 and SPGE-33 resins, while the SPGE-28 material exhibited a slightly lower performance. For the tensile modulus, SPGE-39 and SPGE-33 both exhibited a tensile modulus of 2.8 ± 0.3 GPa, while the tensile modulus of SPGE-28 was 2.3 ± 0.1 GPa.

Meanwhile, the UTS for SPGE-39 and SPGE-33 are 56 ± 2 MPa and 58 ± 1 MPa, respectively, while SPGE-28 exhibits a UTS of 53 ± 1 MPa. As SPGE-28 has the highest amount of reactive diluent present, or BDGE, it is reasonable that it exhibited fewer cross-links and a lower strength. Relative to the BEA resin, the UTS and modulus of the PECAN resin was higher in all cases than BEA resin and comparable to the commercial resin. These results indicate that the PECAN resins are suitable for rigid composite applications.

Finally, the material properties of each formulation are compared with the BEA resin. Overall, all three resins exhibit comparable performance, as presented in Figures 4A–4C, and can be used in FRP applications. Each PECAN resin has unique advantages over the BEA resin. For example, the SPGE-28 formulation possesses a lower fluidity and can be infused faster, while the SPGE-39 resin showed enhanced thermomechanical performance.

Fiberglass composites

FRPs were prepared using the three PECAN resin formulations, the BEA resin, and the Hexion resin via VARTM. Each resin was mixed at a 600 g scale, at the ratios described in Table S3 or as directed by the manufacturer's instructions, and subsequently infused into four-ply unidirectional glass fiber fabric (Saertex unidirectional glass fiber-1,182 g/m²) of approximately 0.3 m × 0.3 m (Figure S3). Resin was infused into the panels to ensure complete coverage, which took approximately 15 min. All infused panels were kept at 80°C for 5 h with a heat blanket to ensure the polymerization reaction went to completion. After infusion, panels were

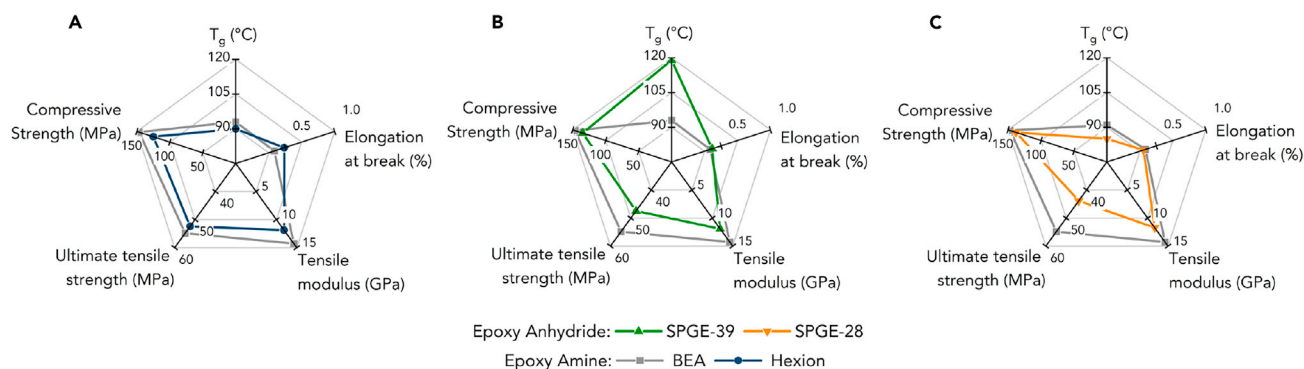


Figure 5. Thermomechanical performance of glass FRPs

(A–C) Spider charts show the T_g , compressive strength, UTS, tensile modulus, and elongation at break for the glass reinforced composites of (A) Hexion, (B) SPGE-39, and (C) SPGE-28 relative to the BEA. Also included in each of these spider charts are data from glass fiber reinforced BEA resin. Temperature-dependent storage modulus and $\tan \delta$ of the FRPs is included in Figure S4. Representative transverse tensile tests (ASTM D3039) and compression tests (ASTM D6641) for all resins are available in Figure S5. Numerical data are provided in Table S5.

removed from the vacuum bags, and samples were cut with a water saw for DMA and tensile testing.

Akin to the neat, cured resin, the FRPs were initially characterized by DMA utilizing a single cantilever fixture perpendicular to the fiber direction. When compared with the neat resin, all PECAN composites exhibit a storage modulus near 6 GPa as the result of the fiber reinforcements and exhibit similar T_g values to the neat polymer resin (Figures S1–S4). Additionally, the approximate three times increase in the storage moduli from the neat resin to the reinforced resin implies stable bonding between the polymer matrix and the glass fiber. The representative BEA resin exhibits near identical behavior to the PECAN system via DMA, with SPGE-33 performing the most similarly due to its similar T_g (Tables S4 and S5).

The resin-fiber interactions were further investigated through mechanical testing, including transverse tension tests (ASTM D3039) and in-plane compression (ASTM D6641) tests conducted in triplicate. Transverse tension tests were conducted perpendicular to the fiber orientation and thus characterized the interface between the resin and fiber. The transverse tension tests revealed that the tensile moduli are 11.9 ± 0.4 GPa, 10.4 ± 0.5 GPa, and 11.7 ± 0.3 GPa, for the SPGE-39, SPGE-33, and SPGE-28 formulas, respectively. Additionally, all three PECAN FRP formulations exhibit a compression strength akin to the epoxy-amine systems at 135 ± 4 MPa, 133 ± 6 MPa, and 138 ± 7 MPa, for the SPGE-39, SPGE-33, and SPGE-28 formulas, respectively, relative to the BEA and Hexion, which possess compressive strengths of 147 ± 7 MPa and 125 ± 7 MPa, respectively (Figure S5 and Table S5). The PECAN FRPs on average exhibit a tensile modulus 4% lower than the BEA FRPs (within the measurement error) and a 10% higher compressive strength (outside of the measurement error).

Finally, the BEA FRP was compared with a Hexion FRP (Figure 5A) and PECAN FRPs (Figure 5B for SPGE-39 and Figure 5C for SPGE-28). The performance of the BEA resin is nearly identical to the Hexion FRP. The Hexion FRP exhibits a slightly greater elongation at break, indicating better fiber adhesion. This result is expected as fiber-glass that is specifically sized for epoxy-amine resins was used. Fracture analysis of the composites via scanning electron microscopy showed excellent adhesion to the Hexion resin and nominal adhesion to the PECAN system (Figure S6). The

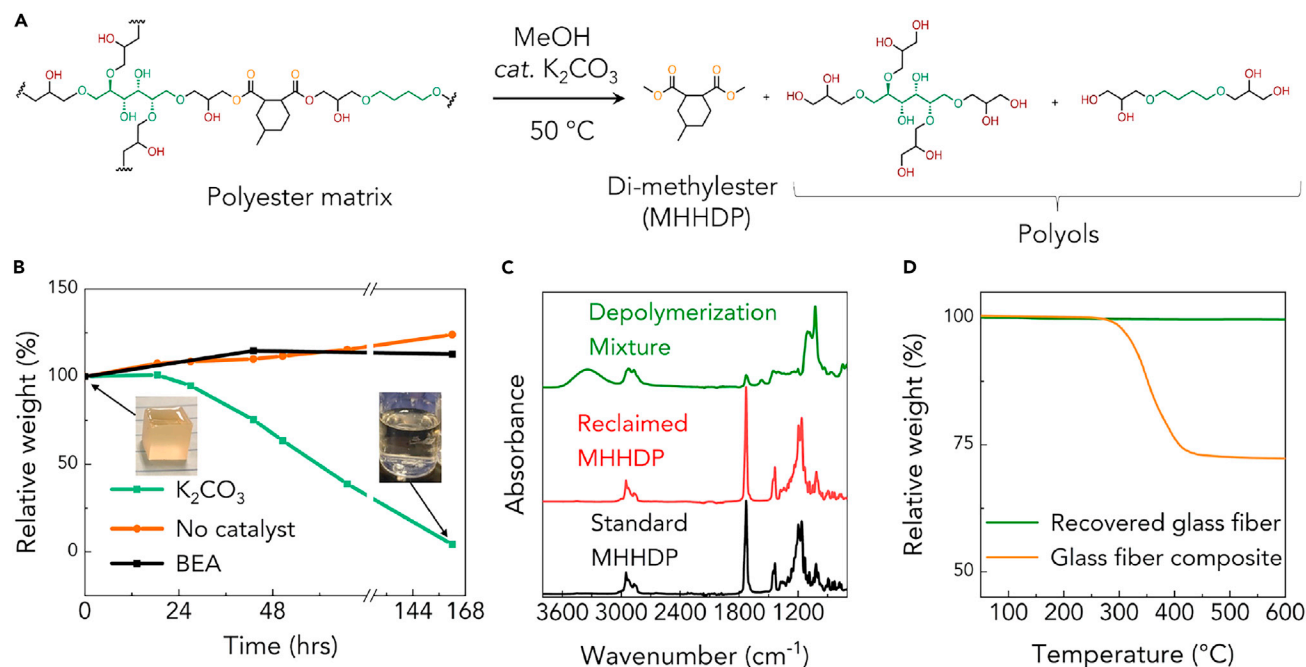


Figure 6. PECAN resin and FRP depolymerization

(A) Depolymerization scheme employed here where K_2CO_3 was used as a catalyst and the reaction was conducted at 50°C for the resin cubes and room temperature for the FRPs.

(B) Depolymerization as a function of time for a 1-g sample in 12 mL MeOH, with and without K_2CO_3 as a catalyst. A 1-g sample of BEA in 12 mL MeOH was also tested.

(C) FTIR spectra demonstrating that the dimethyl ester of MHHPA, MHHDP, can be recovered post depolymerization. Spectra are shown of the depolymerization mixture (top), reclaimed MHHDP from the depolymerization mixture (middle), and of an in-house synthesized standard of MHHDP (bottom).

(D) TGA thermograms of the PECAN FRPs and the glass fiber post depolymerization demonstrating the removal of the PECAN resin. Numerical data are provided in Table S6.

ultimate transverse tensile strength of SPGE-39 is lower than both the baseline and Hexion epoxy-amine FRPs, which is attributed to the fibers being sized for epoxy-amine chemistries. Sizing typically is a chemical modification to the surface of the fibers to ensure interfacial adhesion between the resin and fibers.⁴⁹ Typically, these sizings can be accomplished by functionalizing the fibers with silanes. As an example, the interfacial adhesion could be improved between the fiberglass and PECAN resin the use of (3-mercaptopropyl) trimethoxysilane, which has been previously shown to greatly enhance the interface with polyesters.

PECAN depolymerization

To demonstrate the recyclability of the FRP, base-catalyzed methanolysis was selected to depolymerize the resin.⁵⁰ When subject to methanolysis, the PECAN resin yields methyl esters from the hardener component and polyols from the epoxy components (Figure 6A). The methyl ester is recoverable by distillation and can be converted back to the anhydride, representing a potential 45 wt % recovery for all formulations, while the polyols have the potential to be used directly in subsequent applications, such as polyurethanes.^{51,52} Additionally, the resin represents ~30 wt % of the entire FRPs, and there is the further possibility to reuse the glass fiber (~60 wt % of the FRP) in subsequent FRPs or other applications.

To study the depolymerization, we used potassium carbonate (K_2CO_3) as a catalyst in methanol (MeOH) to depolymerize the PECAN resin. This system, with

dichloromethane as a solvent, has been shown to depolymerize PET at ambient conditions within 24 h.⁵⁰ SPGE-39 was selected as the primary resin to study the depolymerization, as it is the most cross-linked and rigid and thus the most recalcitrant PECAN resin. Initially, neat resin cubes of 1 cm³ in volume were prepared by curing the resin in a silicon tray. The resin cubes were subsequently exposed to 12 mL of MeOH with either 0.05 g K₂CO₃ catalyst or no catalyst at 50°C. Mass measurements were periodically taken to measure reaction progress (Figure 6B and Table S6).

When no catalyst is present, the thermoset only swells in the presence of MeOH, as expected; however, when catalyst is present, the thermoset resin is fully deconstructed after 7 days. After depolymerization, the reaction mixture was subject to FTIR to confirm the presence of the dimethyl ester (Figure 6C). The FTIR spectra of the reaction mixture exhibited broad peaks associated with the presence of polyols (which were not present in the resin spectra) (Figure 3B) and defined regions associated with methylhexahydro-dimethyl phthalate (MHHDP). Additionally, for comparison, a synthesized standard of the dimethyl ester, MHHDP, was prepared (Figure S7) and analyzed via ¹H nuclear magnetic resonance (NMR) spectroscopy. Subsequently, the dimethyl ester was recovered by chromatographic methods, and the FTIR spectra of the separated MHHDP matches the standard. To further demonstrate the circularity of the anhydride, ensuring that it could be used in the same applications, we demonstrated that the dimethyl ester could be hydrolyzed to the diacid (84% yield) and ring-closed to the anhydride (93% yield) (Figure S7) with the potential to further optimize yields. The recycled anhydride has a similar NMR spectrum to the starting anhydride (MHHPA is routinely sold as a mixture of isomers). Additionally, when the recycled anhydride is used alongside fresh epoxies in the SPGE-39 formulation, the resultant resins possess similar thermomechanical properties, specifically a T_g within 3°C.

After work on the neat resin, depolymerization of the FRPs was conducted. The depolymerization was conducted at room temperature in a fume hood without agitation to maintain fiber alignment. Complete dissolution of the polymer was again observed in 7 days (Figure S9). In contrast, an FRP sample made from the typical epoxy-amine matrix showed no sign of degradation. The recovered fiber was washed with MeOH, dried in air, and subjected to TGA (Figure 6D). The reclaimed glass fiber showed 0.6% weight loss when heating from ambient to 600°C, which was comparable with that of the pristine glass fibers (0.7% weight loss at 600°C). Comparatively, the TGA of the FRP demonstrates a 35% weight loss, which is attributed to the resin itself (the composites had approximately 65% fiber weight fraction). Thus, we concluded that the polymer resin was completely removed.

Supply chain and economic modeling

To investigate the economic viability and environmental impacts of the PECAN resin relative to epoxy-amine resins, techno-economic analysis (TEA) and supply chain analysis were conducted to compare the minimum selling price, supply chain energy, and GHG emissions. Due to the complexity of the petrochemical resin formulations and the limited availability of information on their commercial manufacturing, we compared the production of the chemical resin precursors from biological and petrochemical sources, for the bio-derivable PECAN and the petro-derived BEA, respectively. We leveraged existing processes where available, and, in a few cases, constructed process simulations to fill the information gaps. Table S7 details which chemicals models were constructed and which chemicals used an external source, such as the Materials Flow through Industry (MFI) tool^{53,54} or the IHS Chemical

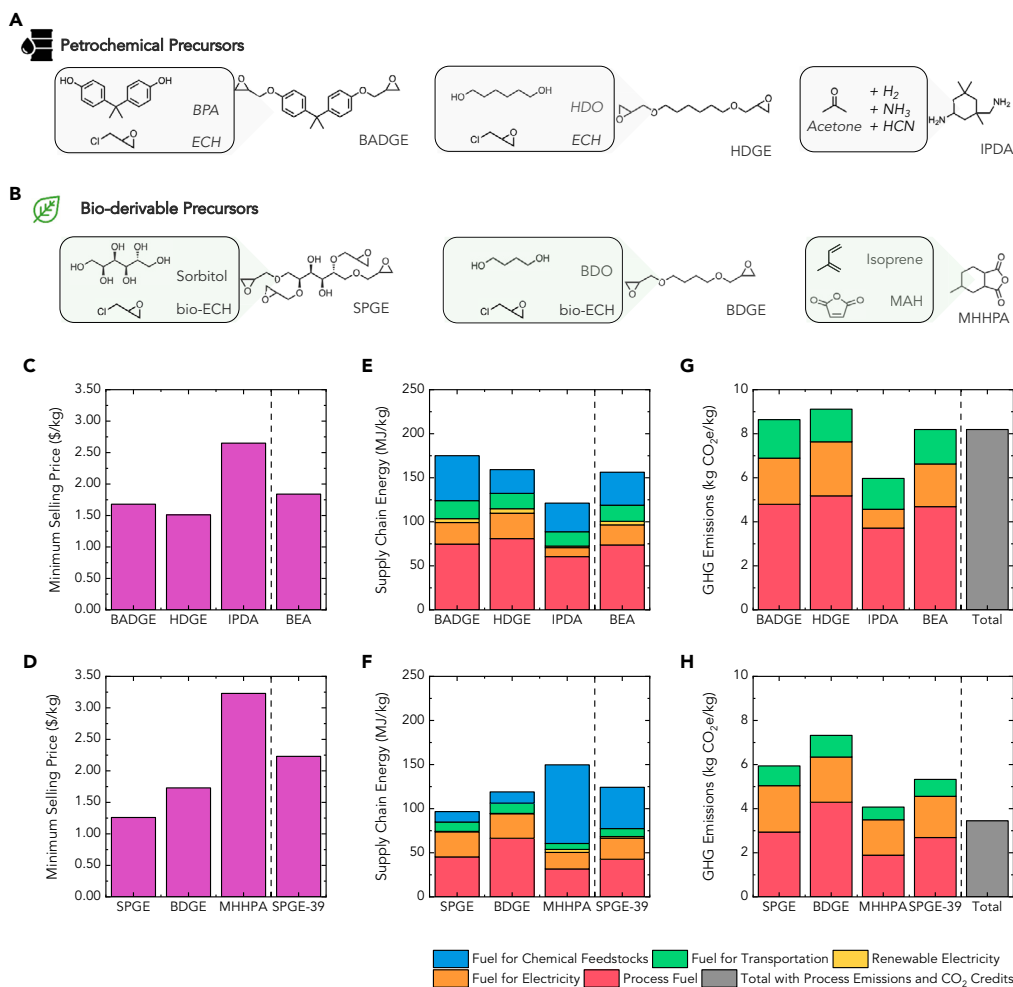


Figure 7. Supply chain and economic analysis of resins

(A) BEA resin precursors and monomers.

(B) PECAN resin precursors and monomers.

(C–F) Supply chain energies for the monomers and resin for both the (C) BEA and (D) PECAN (specifically, SPGE-39). GHG emissions for the monomers and resin for both the (E) BEA and (F) PECAN. Minimum selling price data are provided in Table S9. Numerical data for all formulations are provided in Tables S10 and S11.

Economic Handbook.^{55,56} When models were constructed, Aspen Plus (V10) was used in a manner consistent with the previous analysis.^{41,48,53–64} Importantly, we only modeled the production of the chemical precursors, which we define as one step prior to monomers and two steps prior to the final polymer product. Thus, this analysis excludes the production of the epoxies and hardeners themselves but does include all the relevant inputs in the form of precursors.

For the petrochemically-sourced monomers, BADGE, IPDA, and HDGE, the precursors were bisphenol A, epichlorohydrin (ECH), 1,6-hexanediol (1,6-HDO), isophorone nitrile (IPN), and gray hydrogen (H₂) (Figure 7A). Models were constructed for 1,6-HDO and IPN. Meanwhile, the bio-derived monomers of SPGE, BDGE, and MHPA were combined from precursors of sorbitol, 1,4-BDO, bio-derived ECH (bio-ECH), isoprene, and maleic anhydride, which can all be obtained from bio-based routes (Figure 7B). Sorbitol^{35,36} and maleic anhydride^{39–41} were modeled from the conversion of glucose and xylose, respectively. Bio-ECH was modeled

via the conversion of glycerol, which can be obtained as a by-product of bio-diesel production.^{65–67} Isoprene and 1,4-BDO were both modeled from the direct biological conversion of glucose.^{39–41,68} The bio-derived epoxy monomers are the combination of bio-ECH plus either sorbitol or 1,4-BDO, and MMHPA is formed from the Diels-Alder condensation and hydrogenation of maleic anhydride and isoprene. Further reaction chemistry and process modeling information can be found in [Figures S10 and S11](#) and [Tables S7 and S8](#).

Using this approach, the cost of the BEA resin was estimated to be \$1.84/kg ([Figure 7C](#)), which is lower than the typical epoxy resin (e.g., Hexion) cost of \$2.83/kg.⁵⁴ Both the simplistic formulation of the baseline resin and the assumptions of this model lead to a lower but reasonable estimate. The greatest contributor to cost is IPDA at \$2.65/kg. The bio-derived precursors were modeled at a production capacity of 30 kilotonne per year with a 15% return on investment. The cost of the precursors for the PECAN resin ranges from \$1.23/kg for sorbitol to \$3.48/kg for isoprene, which results in an estimated selling price of \$2.23–2.28/kg across the PECAN formulations ([Figure 7D](#) and [Table S9](#)). Even though this estimate is most likely an underestimate, it was conducted via the same methodology used for the petroleum BEA resin and is found to be within 25% of the estimated price, indicating a potential path to market, especially given its comparable thermomechanical performance alongside the enhanced end-of-life options.

After TEA, the MFI was used to estimate the supply chain energy and GHG emissions of each precursor, monomer, and resin. [Figures 7E and 7F](#) provide the supply chain energy for the BEA and PECAN SPGE-39 monomers and resin, respectively, while the precursors are in [Tables S9 and S10](#). For the BEA, the HDGE requires the most supply chain energy to manufacture (because of the hydrogenation of adipic acid to 1,6-HDO), followed by BADGE. For the PECAN resin, the anhydride hardener, MMHPA, requires the most supply chain energy to manufacture at 150 MJ/kg, which is more than the IPDA hardener for BEA at 121 MJ/kg. Of interest is that the rest of the monomers for the PECAN resin require significantly less supply chain energy than the BEA. Specifically, the SPGE, BDGE, BADGE, and HDGE require 97, 119, 175, and 159 MJ/kg, respectively. When both the BEA and PECAN resins are produced to match the formulations used in this work, the BEA resin requires 156 MJ/kg of supply chain energy, while the PECAN SPGE-39 resin requires 124 MJ/kg, representing an estimated 21% decrease in supply chain energy.

The GHG emissions to produce the precursors, monomers, and resin were also estimated and are provided in [Figures 7G and 7H](#). The same trends that were present in the supply chain energies are also present in the GHG emissions in which the PECAN STGE-39 resin results in a 35% decrease in GHG emissions relative to BEA resin. The greatest contributor to GHG emissions is process fuel, or the fuel necessary to heat the processes. Finally, MFI was used to estimate the GHG emissions after accounting for the CO₂ sequestered during biomass cultivation (Supplemental methods). The full methodology for these calculations is described in the Supplemental materials. Briefly, biogenic CO₂ emissions resulting from the fermentation or combustion of biomass were considered neutral and the biogenic carbon in the final product was taken as a credit. Ultimately, this reduces the GHG emissions by 1.9 kg CO₂-e/kg of PECAN resin ([Figure 7H](#), rightmost bar). When GHG reductions from biomass cultivation are accounted for, the production of the PECAN STGE-39 resin produces 58% less GHG emissions than the BEA resin.

DISCUSSION

Here, we demonstrated that PECAN resins, from bio-derivable epoxies and anhydrides, can serve as a drop-in, recyclable replacement for epoxy-amine resins. The PECAN resin was designed in analogy to the industry standard resin (i.e., Hexion products) by generation of the BEA resin with a rigid monomer, a reactive diluent, and a hardener utilizing monomers that are currently available at scale from various feedstocks. Importantly, the monomers in this work are actively being scaled up by multiple companies (Table S1). Aside from redesigning the chemistry, we examined whether the manufacturability of the resulting FRPs could be maintained, which included ensuring that viscosity of the resultant resins was suitable for an industrially relevant infusion process (VARTM) and that the resins could be subjected to a similar cure schedule as epoxy-amine resins used in composites industries. In addition, we demonstrated comparable, and in some cases favorable, resin and FRP performance alongside end-of-life options with greater than 85% (27 wt % anhydride recovery from the resin, and 60% fiber recovery) possible material recovery. The ability to decarbonize the manufacturing of FRPs was also examined, indicating a greater than 40% potential reduction in supply chain energy and greater than 20% decrease in GHG emissions.

Most of the benefits in this work arise by replacing the amine hardener with an anhydride hardener. Amines are often energy and GHG intensive to manufacture from petrochemical sources.⁶⁹ Additionally, because the MFI tool does not track stoichiometric emissions through the supply chain (e.g., CO₂ resulting from the water gas shift reaction in the steam reforming of natural gas to produce H₂), the overall GHG emissions for virgin epoxy-amine resins are likely higher than reported here. As heteroatom-containing compounds are widely available from biomass-derived feedstocks⁷⁰ and oxygen-containing chemicals can be less energy intense than nitrogen-containing compounds, the use of the bio-derived anhydride hardener contributes to reduced GHG emissions. Although MHPA was shown to be functional in this case, there are multiple anhydrides and carboxylates accessible from biomass that can be used in its place to offer performance tunability.

Other works have previously leveraged epoxy-anhydrides for thermoset redesign.^{24,71–73} These studies demonstrated the applicability of this chemistry and the ability to source the precursor molecules from bio-derived resources, such as epoxidized soybean or tung oil. This work differs from other work as the employed molecules are low-viscosity small molecules, which enables their infusion and high T_g values. When utilizing soybean oil or epoxidized lignin, the resultant materials often exhibit low T_g values⁷⁴ and high viscosities⁷⁵ and would thus require further formulation prior to implementation in rigid composite applications, such as wind turbines, but can still enable their use in other epoxy applications, such as coatings.⁴⁴ Additionally, an epoxy anhydride system, similar to the one developed in this work, has also been implemented in thermosetting systems. Specifically, in the work of Musgrave et al.,⁷⁶ the authors employed a phthalate-based system to enable a higher degree of recyclability and upcycling to photopolymers. Despite these benefits, this work lacks the tunability that is afforded to the multi-component design of this work and implements a toxic and non-bioderivable monomer through the use of phthalates.

In the context of wind turbines, this work demonstrated that a recyclable-by-design resin could be manufactured analogously to the epoxy-amine resin used industrially today. Manufacturability was measured through a similar cure schedule at a 1-kg scale, while the performance was monitored via typical thermomechanical

properties. Going forward, there are further considerations that need to be addressed with scale-up. First, resin cures need to be tested with larger parts with more complex geometries to ensure that the exotherm during polymerization does not result in local overheating, and thus impart defects, while simultaneously ensuring that the cure kinetics do not slow overall throughput. Additionally, fatigue testing on prototypical parts would need to be conducted. This type of scale-up would resemble recent work that has been documented for thermoplastic systems on 13 m blades.²³

Finally, scaled-up recycling of these materials needs to be demonstrated. At the time of writing, there is minimal recycling infrastructure or demonstration of the recycling of thermosets at scale to our knowledge. At larger scales, maintaining fiber orientation will become a challenge and methods that can realign fibers will need to be implemented,^{77,78} second-life applications where orientation does not matter will need to be investigated, or flow-through reactors that maintain fiber alignment will need to be designed. In the case of glass fibers, these processes may not prove to be economical. Thus, there is the opportunity to explore other fibers (e.g., carbon fiber or Kevlar) with greater economic value or to further optimize resin recovery and use across multiple lives will become necessary.

Despite these challenges, advances and learnings from polyester (such as PET) recycling^{14,33,79,80} could be translatable to this work. Additionally, as these materials are used across multiple lives, the decarbonization potential of these materials in subsequent lives could further incentive the adoption of these materials. Multiple life-cycle assessments have demonstrated that the second life of a recyclable-by-design polymer can result in 30% to more than 90% decreases^{48,81} in material cost and GHG emissions for the second life of these materials; thus, similar approaches should be applied to this work. In fact, learnings from PET recycling inform the feasibility of this approach. In a recent publication by Uekert et al.⁸² comparing the TEA and LCA of multiple recycling technologies they estimate the polyester methanolysis would cost \$1.05/kg and emit 4.2 kg-CO₂-e/kg of product for their base case where approximate 80% of products are recovered. Even though further analysis is needed, this result combined with the work conducted here further illustrates the promise of this approach.

Conclusion

Overall, this work demonstrates that bio-derived resins can be designed analogously to today's non-recyclable thermosets to maintain performance and manufacturing while enabling recycling and decarbonization. These benefits are only possible when both the materials performance and processing characteristics are accounted for.

EXPERIMENTAL PROCEDURES

Resource availability

Lead contact

The lead contact for this manuscript is Dr. Nicholas A. Rorrer, who can be contacted at nicholar.rorrer@nrel.gov with any question regarding the manuscript or data sets.

Materials availability

Bisphenol-A di-glycidyl ether and K₂CO₃ were purchased from Sigma-Aldrich. IPDA was purchased from TCI Chemicals. Hexahydro-4-methylphthalic anhydride (a mixture of *cis* and *trans* isomers) was purchased from Sigma-Aldrich and was used for neat resin synthesis. MHHPA was purchased from Broadview Technologies and

used for composite fabrication. Sorbitol-derived tetrafunctional epoxy (Erisys GE-60), 1,4-BDO-derived difunctional epoxy (Erisys GE-21), 1,6-HDO-derived difunctional epoxy (Erisys GE-25), and 2-ethyl-4-methyl imidazole (24EMI) were obtained from CVC Thermoset Specialties, now Huntsman. We obtained 1,200 g/m² unidirectional fiberglass (part number U-E-1,182g/m²-1,500 mm) from Saertex. All reagents were used as received.

Additionally, while the feedstock for the monomers in this work varied widely, multiple companies are actively investing in their scale up from bioderived resources (Table S1).

Data and code availability

All data to reach the conclusions of this manuscript, as well as numerical data for all figures, are provided in the main text or the [supplemental information](#). Data may be made available upon request by contacting the authors directly.

Resin sample synthesis

Neat polymer samples were prepared by mixing the monomers in mass fractions given in Table S2 at the 50-g scale. The mixed resin was placed under vacuum for 30 min to remove air and prevent the formation of bubbles. Subsequently, the resin was casted into molds with a desired geometry (e.g., rectangular DMA bars, tensile test specimen), and the cast resin was cured in an oven at 80°C for 5 h.

Fabrication of FRPs

Resin mixtures were homogenized by hand stirring and were subsequently degassed for 15 min under vacuum. The resin was then infused, via a tube, to four layers of fiber that were horizontally laid on a glass surface. For 1 ft² panels, an infusion time of ~15 min was observed for the PECAN and BEA resins to fully wet the fibers. The infused resin was cured by applying a heating blanket that was set at 80°C for 5 h. Last, the composites were cut into desired test specimens for mechanical testing via a diamond saw.

Chemical characterization

FTIR spectroscopy

A single reflectance attenuated total reflection setup was used on a Thermo 6700 spectrometer. The curing reaction was monitored by the shift of carbonyl vibration from the anhydride to the ester.

NMR spectroscopy

A Bruker Avance 400-MHz spectrometer equipped with a 5-mm BBO probe was used to collect ¹H NMR spectra. Spectra were collected across at least 64 scans at a relaxation time of 30 s.

Thermomechanical characterization

DMA

Samples with approximately 30 mm (length) × 12 mm (width) × 2 mm (depth) were loaded by a single cantilever clamp on a TA Q800 DMA and were monitored over an oscillatory strain of 0.1% at 1 Hz, from 35°C to 180°C at 3°C/min. The T_g was measured at the highest point on the tan δ curve.

DSC

Samples (~10 mg) were loaded by an aluminum pan on a TA Q2000 with an auto-sampler. A first heating cycle was used to erase thermal history. The T_g was

determined by extrapolating the middle point of the step that was observed in the second heating cycle.

TGA

Samples with 5–10 mg in mass were monitored on a TA Q500. A temperature ramp of 20°C/min was applied until 600°C. The samples were under nitrogen throughout the test unless otherwise noted.

Tensile and compression testing

All tension and compression tests were performed on an MTS 100 kN servo-hydraulic load frame with MTS FlexTest 40 and Multipurpose Elite software. Neat resin tensile mechanical properties were obtained by following ASTM D638-14 “Standard Test Method for Tensile Properties of Plastics” with type IV dog bone specimens. Transverse tension and transverse compression testing were selected for initial composite characterization due to the resin-dominant failure modes represented in these tests. They were decided to be the most appropriate tests to assess the compatibility of the polymer resin systems with the glass reinforcements. Transverse tension tests were conducted following ASTM D3039 “Standard Test Method for Tensile Properties of Polymer Matrix Composite Materials,” with a modified dog bone specimen geometry with a total length of 200-mm and gage section of 60 mm (length) × 5 mm (width) to minimize gripping effects and encourage failure within the gage section. Strains for all tension testing were measured using an MTS extensometer with a 25-mm gage length. Compression strengths were obtained by following ASTM D6641 “Standard Test Method for Compressive Properties of Polymer Matrix Composite Materials Using a Combined Loading Compression (CLC) Test Fixture.” Strains were measured using bonded foil strain gages.

TEA and supply chain analysis

A majority of the background on the process models are provided in the SI. The general approach taken follows that of previous work published in our group.⁶⁴ Briefly, chemical process models were developed in AspenPlus version 10 to produce the chemical precursors with information based on the peer-reviewed literature and IHS Chemical Economics Handbook.^{55,56}

The life cycle inventory from the production of the precursors was subsequently exported into MFI to perform supply chain analysis, in a manner also consistent with our previous.^{48,54,63,64,69} Basics of the MFI tool can be found in Hanes and Carpenter⁵³ and this work was conducted by utilizing version 2.2 of the MFI tool (mfifool.nrel.gov).

SUPPLEMENTAL INFORMATION

Supplemental information can be found online at <https://doi.org/10.1016/j.matt.2023.10.033>.

ACKNOWLEDGMENTS

This work was authored by the National Renewable Energy Laboratory, operated by Alliance for Sustainable Energy, LLC, for the U.S. Department of Energy (DOE) under contract no. DE-AC36-08GO28308. Funding for N.A.R., E.G.R., and G.T.B. was provided in part by U.S. Department of Energy Office of Energy Efficiency and Vehicles Technologies Office. C.W., R.M., N.A.R., P.M., R.B., D.B., G.T.B., and R.D.A. were supported in part by the Laboratory Directed Research and Development (LDRD)

Program at NREL. Additionally, funding for some components of this work was provided by the U.S. Department of Energy, Office of Energy Efficiency and Renewable Energy, Advanced Materials and Manufacturing Technologies Office (AMMTO) and Bioenergy Technologies Office (BETO) as part of the BOTTLE Consortium, supported by AMMTO and BETO under contract no. DE-AC36-08GO28308 with the National Renewable Energy Laboratory, operated by Alliance for Sustainable Energy, LLC. The views expressed in the article do not necessarily represent the views of the DOE or the U.S. Government.

AUTHOR CONTRIBUTIONS

Funding acquisition: N.A.R., R.M., and G.T.B.; conceptualization: C.W., R.M., N.A.R., and G.T.B.; investigation: C.W., A.S., E.G.R., R.M., G.M., M.S., P.M., J.D., S.R.N., K.H., R.C., F.M., A.J.S., D.B., and R.B.; methodology: C.W., R.M., A.S., N.A.R., and G.T.B.; supervision: R.M., N.A.R., and G.T.B.; visualization: C.W., E.G.R., and N.A.R.; writing – original draft: C.W. and R.M.; writing – review and editing: N.A.R., A.S., E.G.R., and G.T.B.

DECLARATION OF INTERESTS

C.W., E.G.R., R.M., R.D.A., N.A.R., and G.T.B. have submitted a patent application on recyclable-by-design materials.

INCLUSION AND DIVERSITY

One or more of the authors of this paper self-identifies as an underrepresented ethnic minority in their field of research or within their geographical location. One or more of the authors of this paper self-identifies as a gender minority in their field of research. One or more of the authors of this paper self-identifies as a member of the LGBTQ+ community. While citing references scientifically relevant for this work, we also actively worked to promote gender balance in our reference list.

Received: June 18, 2023

Revised: October 1, 2023

Accepted: October 31, 2023

Published: December 5, 2023

REFERENCES

- Pham, H.Q., and Marks, M.J. (2005). Epoxy Resins. *Ullmann's Encycl. Ind. Chem.*
- Lubin, G. (2013). *Handbook of Composites* (Springer Science & Business Media).
- Kandelbauer, A., Tondi, G., Zaske, O.C., and Goodman, S.H. (2014). Unsaturated Polyesters and Vinyl Esters. In *Handbook of Thermoset Plastics*, H. Dodiuk and S.H. Goodman, eds. (William Andrew Publishing), pp. 111–172.
- Sathishkumar, T.P., Satheshkumar, S., and Naveen, J. (2014). Glass fiber-reinforced polymer composites – a review. *J. Reinf. Plast. Compos.* 33, 1258–1275.
- Linak, E., Buchholz, U., Guan, M., and Kishi, A. (2018). Epoxy Resins (IHS Markit).
- Liu, P., and Barlow, C.Y. (2017). Wind turbine blade waste in 2050. *Waste Manag.* 62, 229–240.
- Naqvi, S.R., Prabhakara, H.M., Bramer, E.A., Dierkes, W., Akkerman, R., and Brem, G. (2018). A critical review on recycling of end-of-life carbon fibre/glass fibre reinforced composites waste using pyrolysis towards a circular economy. *Resour. Conserv. Recycl.* 136, 118–129.
- Wang, Y., Cui, X., Ge, H., Yang, Y., Wang, Y., Zhang, C., Li, J., Deng, T., Qin, Z., and Hou, X. (2015). Chemical Recycling of Carbon Fiber Reinforced Epoxy Resin Composites via Selective Cleavage of the Carbon–Nitrogen Bond. *ACS Sustainable Chem. Eng.* 3, 3332–3337.
- Ma, Y., and Nutt, S. (2018). Chemical treatment for recycling of amine/epoxy composites at atmospheric pressure. *Polym. Degrad. Stab.* 153, 307–317.
- Navarro, C.A., Ma, Y., Michael, K.H., Breunig, H.M., Nutt, S.R., and Williams, T.J. (2021). Catalytic, aerobic depolymerization of epoxy thermoset composites. *Green Chem.* 23, 6356–6360.
- McBride, M.K., Worrell, B.T., Brown, T., Cox, L.M., Sowan, N., Wang, C., Podgorski, M., Martinez, A.M., and Bowman, C.N. (2019). Enabling Applications of Covalent Adaptable Networks. *Annu. Rev. Chem. Biomol. Eng.* 10, 175–198.
- Denissen, W., Winne, J.M., and Du Prez, F.E. (2016). Vitrimers: permanent organic networks with glass-like fluidity. *Chem. Sci.* 7, 30–38.
- Korley, L.T.J., Epps, T.H., 3rd, Helms, B.A., and Ryan, A.J. (2021). Toward polymer upcycling—adding value and tackling circularity. *Science* 373, 66–69.
- George, N., and Kurian, T. (2014). Recent Developments in the Chemical Recycling of Postconsumer Poly(ethylene terephthalate) Waste. *Ind. Eng. Chem. Res.* 53, 14185–14198.
- Suematsu, K., Nakamura, K., and Takeda, J. (1983). Polyimine, a C=N Double Bond Containing Polymers: Synthesis and Properties. *Polym. J.* 15, 71–79.

16. Geng, H., Wang, Y., Yu, Q., Gu, S., Zhou, Y., Xu, W., Zhang, X., and Ye, D. (2018). Vanillin-Based Polyschiff Vitrimers: Reprocessability and Chemical Recyclability. *ACS Sustainable Chem. Eng.* 6, 15463–15470.
17. Christensen, P.R., Scheuermann, A.M., Loeffler, K.E., and Helms, B.A. (2019). Closed-loop recycling of plastics enabled by dynamic covalent diketoenamine bonds. *Nat. Chem.* 11, 442–448.
18. Taynton, P., Ni, H., Zhu, C., Yu, K., Loob, S., Jin, Y., Qi, H.J., and Zhang, W. (2016). Repairable woven carbon fiber composites with full recyclability enabled by malleable polyimine networks. *Adv. Mater.* 28, 2904–2909.
19. Wang, S., Yang, Y., Ying, H., Jing, X., Wang, B., Zhang, Y., and Cheng, J. (2020). Recyclable, Self-Healable, and Highly Malleable Poly(urethane-urea)s with Improved Thermal and Mechanical Performances. *ACS Appl. Mater. Interfaces* 12, 35403–35414.
20. Wang, C., Goldman, T.M., Worrell, B.T., McBride, M.K., Alim, M.D., and Bowman, C.N. (2018). Recyclable and repolymerizable thiol–X photopolymers. *Mater. Horiz.* 5, 1042–1046.
21. Cui, C., Chen, X., Ma, L., Zhong, Q., Li, Z., Mariappan, A., Zhang, Q., Cheng, Y., He, G., Chen, X., et al. (2020). Polythiourethane Covalent Adaptable Networks for Strong and Reworkable Adhesives and Fully Recyclable Carbon Fiber-Reinforced Composites. *ACS Appl. Mater. Interfaces* 12, 47975–47983.
22. Veers, P., Dykes, K., Lantz, E., Barth, S., Bottasso, C.L., Carlson, O., Clifton, A., Green, J., Green, P., Holttinen, H., et al. (2019). Grand challenges in the science of wind energy. *Science* 366, eaau2027.
23. Murray, R.E., Beach, R., Barnes, D., Snowberg, D., Berry, D., Rooney, S., Jenks, M., Gage, B., Boro, T., Wallen, S., and Hughes, S. (2021). Structural validation of a thermoplastic composite wind turbine blade with comparison to a thermoset composite blade. *Renew. Energy* 164, 1100–1107.
24. Ding, C., and Matharu, A.S. (2014). Recent Developments on Biobased Curing Agents: A Review of Their Preparation and Use. *ACS Sustainable Chem. Eng.* 2, 2217–2236.
25. Han, J., Liu, T., Hao, C., Zhang, S., Guo, B., and Zhang, J. (2018). A Catalyst-Free Epoxy Vitrimer System Based on Multifunctional Hyperbranched Polymer. *Macromolecules* 51, 6789–6799.
26. Ma, Z., Wang, Y., Zhu, J., Yu, J., and Hu, Z. (2017). Bio-based epoxy vitrimers: Reprocessability, controllable shape memory, and degradability. *J. Polym. Sci., Part A: Polym. Chem.* 55, 1790–1799.
27. Baroncini, E.A., Kumar Yadav, S., Palmese, G.R., and Stanzione, J.F. (2016). Recent advances in bio-based epoxy resins and bio-based epoxy curing agents. *J. Appl. Polym. Sci.* 133.
28. Stadler, B.M., Wulf, C., Werner, T., Tin, S., and de Vries, J.G. (2019). Catalytic Approaches to Monomers for Polymers Based on Renewables. *ACS Catal.* 9, 8012–8067.
29. Montazeri, M., Zaimes, G.G., Khanna, V., and Eckelman, M.J. (2016). Meta-Analysis of Life Cycle Energy and Greenhouse Gas Emissions for Priority Biobased Chemicals. *ACS Sustainable Chem. Eng.* 4, 6443–6454.
30. Garcia, J.M., and Robertson, M.L. (2017). The future of plastics recycling. *Science* 358, 870–872.
31. Martín, A.J., Mondelli, C., Jaydev, S.D., and Pérez-Ramírez, J. (2021). Catalytic processing of plastic waste on the rise. *Chem* 7, 1487–1533.
32. Ellis, L.D., Rorrer, N.A., Sullivan, K.P., Otto, M., McGeehan, J.E., Román-Leshkov, Y., Wierckx, N., and Beckham, G.T. (2021). Chemical and biological catalysis for plastics recycling and upcycling. *Nat. Catal.* 4, 539–556.
33. Allen, R.D., and James, M.I. (2021). Chemical Recycling of PET. In *Circular Economy of Polymers: Topics in Recycling Technologies* (American Chemical Society), pp. 61–80.
34. Inc, H. (2006). EPIKOTE™ Resin MGS™ RIMR 135 and EPIKURE™ Curing Agent MGS™ RIMH 134–RIMH 137.
35. de Jong, E., Higson, A., Walsh, P., and Wellisch, M. (2012). Product developments in the bio-based chemicals arena. *Biofuel. Bioprod. Biorefin.* 6, 606–624.
36. Zheng, M., Pang, J., Sun, R., Wang, A., and Zhang, T. (2017). Selectivity Control for Cellulose to Diols: Dancing on Eggs. *ACS Catal.* 7, 1939–1954.
37. Yim, H., Haselbeck, R., Niu, W., Pujol-Baxley, C., Burgard, A., Boldt, J., Khandurina, J., Trawick, J.D., Osterhout, R.E., Stephen, R., et al. (2011). Metabolic engineering of *Escherichia coli* for direct production of 1,4-butanediol. *Nat. Chem. Biol.* 7, 445–452.
38. Burgard, A., Burk, M.J., Osterhout, R., Van Dien, S., and Yim, H. (2016). Development of a commercial scale process for production of 1,4-butanediol from sugar. *Curr. Opin. Biotechnol.* 42, 118–125.
39. Bechthold, I., Bretz, K., Kabasci, S., Kopitzky, R., and Springer, A. (2008). Succinic Acid: A New Platform Chemical for Biobased Polymers from Renewable Resources. *Chem. Eng. Technol.* 31, 647–654.
40. Chung, H., Yang, J.E., Ha, J.Y., Chae, T.U., Shin, J.H., Gustavsson, M., and Lee, S.Y. (2015). Bio-based production of monomers and polymers by metabolically engineered microorganisms. *Curr. Opin. Biotechnol.* 36, 73–84.
41. Kumamoto, T., Bland, A., Greiner, E., and Zhang, Y. (2019). 1,4-Butanediol (IHS Markit).
42. Cok, B., Tsiropoulos, I., Roes, A.L., and Patel, M.K. (2013). Succinic acid production derived from carbohydrates: An energy and greenhouse gas assessment of a platform chemical toward a bio-based economy. *Biofuel. Bioprod. Biorefin.* 8, 16–29.
43. Wojcieszak, R., Santarelli, F., Paul, S., Dumeignil, F., Cavani, F., and Gonçalves, R.V. (2015). Recent developments in maleic acid synthesis from bio-based chemicals. *Sustain. Chem. Process.* 3, 9.
44. Linak, E., Buchholz, U., Guan, M., and Kishi, A. (2017). Epoxy Surface Coatings (IHS).
45. Massingill, J.L., and Bauer, R.S. (2000). Epoxy Resins. In *Applied Polymer Science: 21st Century*, C.D. Craver and C.E. Carraher, eds. (Pergamon), pp. 393–424.
46. Tziamtzi, C.K., and Chrissafis, K. (2021). Optimization of a commercial epoxy curing cycle via DSC data kinetics modelling and TTT plot construction. *Polymer* 230, 124091.
47. Rorrer, N.A., Vardon, D.R., Dorgan, J.R., Gjersing, E.J., and Beckham, G.T. (2017). Biomass-derived monomers for performance-differentiated fiber reinforced polymer composites. *Green Chem.* 19, 2812–2825.
48. Rorrer, N.A., Nicholson, S., Carpenter, A., Biddy, M.J., Grundl, N.J., and Beckham, G.T. (2019). Combining Reclaimed PET with Bio-based Monomers Enables Plastics Upcycling. *Joule* 3, 1006–1027.
49. Thomason, J.L. (2019). Glass fibre sizing: A review. *Compos. Appl. Sci. Manuf.* 127, 105619.
50. Pham, D.D., and Cho, J. (2021). Low-energy catalytic methanolysis of poly(ethyleneterephthalate). *Green Chem.* 23, 511–525.
51. Nohra, B., Candy, L., Blanco, J.-F., Guerin, C., Raoul, Y., and Mouloungui, Z. (2013). From Petrochemical Polyurethanes to Biobased Polyhydroxyurethanes. *Macromolecules* 46, 3771–3792.
52. Akindoyo, J.O., Beg, M.D.H., Ghazali, S., Islam, M.R., Jeyaratnam, N., and Yuvaraj, A.R. (2016). Polyurethane types, synthesis and applications – a review. *RSC Adv.* 6, 114453–114482.
53. Hanes, R.J., and Carpenter, A. (2017). Evaluating opportunities to improve material and energy impacts in commodity supply chains. *Environ. Syst. Decis.* 37, 6–12.
54. Nicholson, S.R., Rorrer, N.A., Carpenter, A.C., and Beckham, G.T. (2021). Manufacturing energy and greenhouse gas emissions associated with plastics consumption. *Joule* 5, 673–686.
55. (2016). *Chemical Economics Handbook*. <https://news.ihsmarket.com>.
56. *Process Economics Program Yearbook*. (2019).
57. Atreja, P., and Smith, K. (2022). Acetone (IHS Markit).
58. Guan, M., Buchholz, U., Kishi, A., and Linak, E. (2021). Epichlorohydrin (IHS Markit).
59. Kumamoto, T., Bland, A., Greiner, E., and Zhang, Y. (2021). Alkylamines (C1–C6) (IHS Markit).
60. Monconduit, M., and Smith, K. (2021). Cyclohexanol and Cyclohexanone (IHS Markit).
61. Ormonde, E., Yoneyama, M., and Zhu, X. (2020). Isoprene (IHS Markit).
62. Pampell, M. (2020) (Bisphenol-A. IHS Markit).
63. Rorrer, N.A., Notonier, S.F., Knott, B.C., Black, B.A., Singh, A., Nicholson, S.R., Kinchin, C.P., Schmidt, G.P., Carpenter, A.C., Ramirez, K.J., et al. (2022). Production of β -ketoacid from glucose in *Pseudomonas putida* KT2440 for use in performance-advantaged nylons. *Cell Reports Physical Science* 3, 100840.

64. Singh, A., Rorrer, N.A., Nicholson, S.R., Erickson, E., DesVeaux, J.S., Avelino, A.F., Lamers, P., Bhatt, A., Zhang, Y., Avery, G., et al. (2021). Techno-economic, life-cycle, and socioeconomic impact analysis of enzymatic recycling of poly(ethylene terephthalate). *Joule* 5, 2479–2503.
65. Adom, F., Dunn, J.B., Han, J., and Sather, N. (2014). Life-cycle fossil energy consumption and greenhouse gas emissions of bioderived chemicals and their conventional counterparts. *Environ. Sci. Technol.* 48, 14624–14631.
66. Sheldon, R.A. (2014). Green and sustainable manufacture of chemicals from biomass: state of the art. *Green Chem.* 16, 950–963.
67. Bell, B.M., Briggs, J.R., Campbell, R.M., Chambers, S.M., Gaarenstroom, P.D., Hippler, J.G., Hook, B.D., Kearns, K., Kenney, J.M., Kruper, W.J., et al. (2008). Glycerin as a Renewable Feedstock for Epichlorohydrin Production. The GTE Process. *CLEAN Soil Air Water* 36, 657–661.
68. Gräffe, H., Körnig, W., Weitz, H.-M., Reiß, W., Steffan, G., Diehl, H., Bosche, H., Schneider, K., Kieczka, H., and Pinkos, R. (2019). Butanediols, Butenediol, and Butynediol. *Ullmann's encycl. ind. chem.* 1–12.
69. Nicholson, S.R., Rorrer, N.A., Uekert, T., Avery, G., Carpenter, A.C., and Beckham, G.T. (2023). Manufacturing energy and greenhouse gas emissions associated with United States consumption of organic petrochemicals. *ACS Sustainable Chem. Eng.* 11, 2198–2208.
70. Cywar, R.M., Rorrer, N.A., Hoyt, C.B., Beckham, G.T., and Chen, E.Y.-X. (2021). Bio-based polymers with performance-advantaged properties. *Nat. Rev. Mater.* 7, 83–103.
71. Zhang, Q., Molenda, M., and Reineke, T.M. (2016). Epoxy Resin Thermosets Derived from Trehalose and β -Cyclodextrin. *Macromolecules* 49, 8397–8406.
72. Llevot, A., Grau, E., Carlotti, S., Grelier, S., and Cramail, H. (2016). From Lignin-derived Aromatic Compounds to Novel Biobased Polymers. *Macromol. Rapid Commun.* 37, 9–28.
73. Xin, J., Li, M., Li, R., Wolcott, M.P., and Zhang, J. (2016). Green Epoxy Resin System Based on Lignin and Tung Oil and Its Application in Epoxy Asphalt. *ACS Sustainable Chem. Eng.* 4, 2754–2761.
74. Kumar, S., Samal, S.K., Mohanty, S., and Nayak, S.K. (2017). Epoxidized Soybean Oil-Based Epoxy Blend Cured with Anhydride-Based Cross-Linker: Thermal and Mechanical Characterization. *Ind. Eng. Chem. Res.* 56, 687–698.
75. Adhvaryu, A., and Erhan, S.Z. (2002). Epoxidized soybean oil as a potential source of high-temperature lubricants. *Ind. Crop. Prod.* 15, 247–254.
76. Musgrave, G.M., Bishop, K.M., Kim, J.S., Heiner, A.C., and Wang, C. (2023). Polyester networks from structurally similar monomers: recyclable-by-design and upcyclable to photopolymers. *Polym. Chem.* 14, 2964–2970.
77. Harper, L.T., Turner, T.A., Martin, J.R.B., and Warrior, N.A. (2008). Fiber Alignment in Directed Carbon Fiber Preforms — A Feasibility Study. *J. Compos. Mater.* 43, 57–74.
78. van de Werken, N., Reese, M.S., Taha, M.R., and Tehrani, M. (2019). Investigating the effects of fiber surface treatment and alignment on mechanical properties of recycled carbon fiber composites. *Composites Part A* 119, 38–47.
79. Khoonkari, M., Haghghi, A.H., Sefidbakht, Y., Shekoochi, K., and Ghaderian, A. (2015). Chemical Recycling of PET Wastes with Different Catalysts. *Int. J. Polym. Sci.* 2015, 1–11.
80. Sinha, V., Patel, M.R., and Patel, J.V. (2008). Pet Waste Management by Chemical Recycling: A Review. *J. Polym. Environ.* 18, 8–25.
81. Christensen, P.R., Scheuermann, A.M., Loeffler, K.E., and Helms, B.A. (2019). Closed-loop recycling of plastics enabled by dynamic covalent diketoenamine bonds. *Nat. Chem.* 11, 442–448.
82. Uekert, T., Singh, A., DesVeaux, J.S., Ghosh, T., Bhatt, A., Yadav, G., Afzal, S., Walzberg, J., Knauer, K.M., Nicholson, S.R., Technical, et al. (2023). Economic, and Environmental Comparison of Closed-Loop Recycling Technologies for Common Plastics. *ACS Sustainable Chem. Eng.* 11, 965–978.